

## Raman and ARPES combined study on the connection between the existence of the pseudogap and the topology of the Fermi surface in $\text{Bi}_2\text{Sr}_2\text{CaCu}_2\text{O}_{8+\delta}$

B. Loret,<sup>1</sup> Y. Gallais,<sup>1</sup> M. Cazayous,<sup>1</sup> R. D. Zhong,<sup>2</sup> J. Schneeloch,<sup>2</sup> G. D. Gu,<sup>2</sup> A. Fedorov,<sup>3</sup> T. K. Kim,<sup>4</sup> S. V. Borisenko,<sup>3</sup> and A. Sacuto<sup>1</sup>

<sup>1</sup>Laboratoire Matériaux et Phénomènes Quantiques (UMR 7162 CNRS), Université Paris Diderot-Paris 7, Bat. Condorcet, 75205 Paris Cedex 13, France

<sup>2</sup>Matter Physics and Materials Science, Brookhaven National Laboratory (BNL), Upton, New York 11973, USA

<sup>3</sup>IFW-Dresden, Helmholtzstrasse 20, 01069 Dresden, Germany

<sup>4</sup>Diamond Light Source, Harwell Campus, Didcot OX11 0DE, United Kingdom



(Received 31 January 2018; revised manuscript received 26 March 2018; published 30 May 2018)

We study the behavior of the pseudogap in overdoped  $\text{Bi}_2\text{Sr}_2\text{CaCu}_2\text{O}_{8+\delta}$  by electronic Raman scattering (ERS) and angle-resolved photoemission spectroscopy (ARPES) on the same single crystals. Using both techniques we find that, unlike the superconducting gap, the pseudogap related to the antibonding band vanishes above the critical doping  $p_c = 0.22$ . Concomitantly, we show from ARPES measurements that the Fermi surface of the antibonding band is holelike below  $p_c$  and becomes electronlike above  $p_c$ . This reveals that the existence of the pseudogap depends on the Fermi surface topology in  $\text{Bi}_2\text{Sr}_2\text{CaCu}_2\text{O}_{8+\delta}$ , and more generally, puts strong constraint on theories of the pseudogap phase.

DOI: [10.1103/PhysRevB.97.174521](https://doi.org/10.1103/PhysRevB.97.174521)

### I. INTRODUCTION

Revealing the true nature of the pseudogap (PG) phase remains one of the main challenges for understanding physics of hole doped copper oxide superconductors. After several decades of research, key elements still emerge without being able to identify the origin of the PG. The PG sets below a characteristic temperature  $T^*(p)$  which is a decreasing function of the doping  $p$ . It manifests by a loss of low-energy spectral weight in many different probes [1–13] with electronic broken-symmetry states [14–19]. There is now an increasing number of compelling experimental evidences that the PG also develops below the superconducting transition temperature  $T_c$  [5,16–18,20–26]. Rather than trying to determine the origin of the PG phase which remains a difficult task, we propose an alternative approach which consists of finding the conditions of its survival. In our previous investigations, we showed the PG phase collapses abruptly in the overdoped regime of  $\text{Bi}_2\text{Sr}_2\text{CaCu}_2\text{O}_{8+\delta}$  (Bi-2212) close to  $p_c = 0.22$  and its end draws a vertical line under the superconducting dome in the  $T$ - $p$  phase diagram [13,26]. This observation should be related to the anisotropy disappearance of the scattering rate reported earlier at the same doping [27]. We showed the PG collapse coincides with a sharp peak in the density of states (DOS) of the underlying band structure around the antinodal region of the Brillouin zone [13]. By using ARPES data obtained from Bi-2212 at high doping levels which observed a change of the Fermi surface (FS) topology [28], we have interpreted the enhancement of the DOS as the manifestation of a doping induced Lifshitz quantum phase transition wherein, as a van Hove singularity crosses the chemical potential, the active holelike antibonding Fermi surface of bilayer Bi-2212 becomes electronlike while the bonding band remains holelike [13]. These results suggested indirectly that the PG end in Bi-2212 is due to a change of the FS topology. Note that the Raman response

is predominantly sensitive to the antibonding band since the latter is close to a density of states singularity which strongly enhances the Raman response as reported in our previous investigations [13]. It is generally believed then that the information about the possible existence of a pseudogap in the bonding band is preempted by the large antibonding band response.

A possible link between the PG and the Fermi surface topology in cuprates was also inferred from previous works on  $\text{La}_{2-x}\text{Sr}_x\text{CuO}_4$  (LSCO) [29–31] and its related compounds  $\text{Nd}_{0.4}\text{Sr}_x\text{CuO}_4$  (Nd-LSCO) [32] and  $\text{Bi}_2\text{Sr}_2\text{CuO}_{6+\delta}$  (Bi-2201) [33,34].

More recently, a detailed study on low-temperature high-magnetic-field transport measurements under pressure in the Nd-LSCO system infers that the PG cannot open on an electronlike Fermi surface [35]. This is confirmed by two recent theoretical studies in the framework of a two-dimensional Hubbard model. They showed that a PG only opens on holelike Fermi surfaces for a wide range of band structure parameters, even in the strong-coupling regime where the antiferromagnetic correlations responsible for the PG are short ranged [36,37].

In order to demonstrate unambiguously that the change of the FS topology actually exists, it is not an accident and indeed plays a key role in the disappearance of the PG in Bi-2212, we have combined ARPES and ERS measurements on the same single crystals at high doping levels to check that both the ERS and ARPES signatures of the PG disappear simultaneously when the antibonding band of the FS becomes electronlike.

### II. COMBINED RAMAN AND ARPES EXPERIMENTS

Our studies are focused on two Bi-2212 overdoped single crystals OD 47 K ( $p = 0.236$ ) and OD 77 K ( $p = 0.201$ ), respectively, located below and above the Lifshitz transition which is located close to  $p_c = 0.22$ .

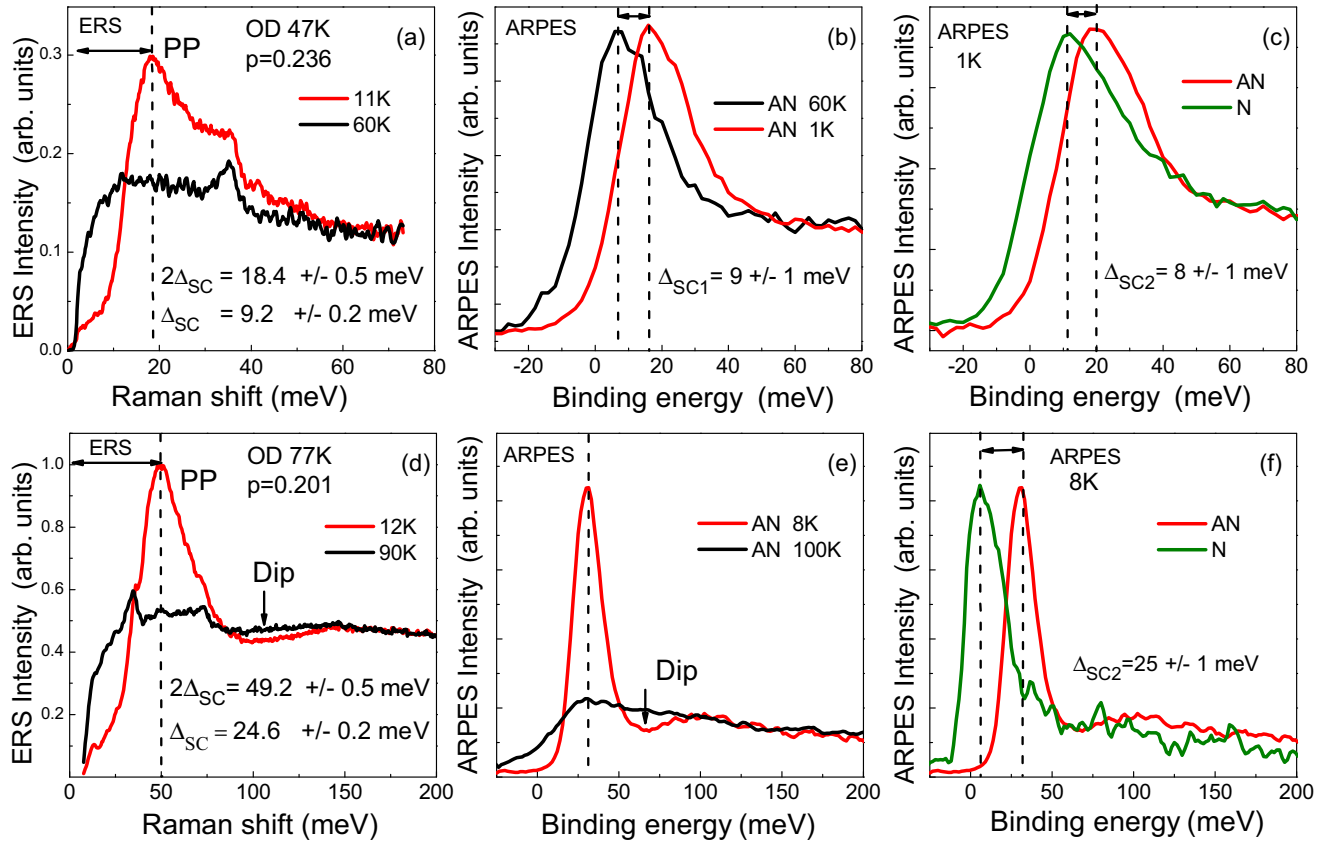


FIG. 1. First row: ERS and ARPES spectra of Bi-2212 overdoped (OD 47 K) crystal above  $p_c = 0.22$ : (a)  $B_{1g}$  (antinodal) Raman response, (b) antinodal EDCs of the antibonding band below and above  $T_c$ , and (c) antinodal and nodal EDCs of the antibonding band below  $T_c$ . Note that the EDCs have been selected to emphasize momentum and temperature dependence, respectively. The antinodal EDC from (c) is a little broader than the one in (b) and this caused a slightly higher binding energy of the peak. For the gap determination this difference plays no role since it is relative changes of the line shape which are important. Second row: ERS and ARPES spectra of Bi-2212 overdoped (OD 77 K) crystal below  $p_c$ : (d) antinodal Raman response, (e) antinodal EDCs of the antibonding band below and above  $T_c$ , and (f) antinodal and nodal EDCs of the antibonding band below  $T_c$ . The peak at 35 and weak reminiscent peaks at 50 and 75 meV observed both in (a) and (d) are phonon lines [41,42]. Zero binding energy corresponds to the Fermi level.

The doping level was estimated from the pair breaking peak location detected in the Raman spectra [38]. The doping estimate from ARPES (although less accurate due to many diffraction replicas) is consistent with that of Raman. We find from Luttinger's theorem:  $p = 0.24 \pm 0.01$  for the OD 47 K compound and  $p = 0.21 \pm 0.01$  for the OD 77 K compound.

Raman experiments have been carried out using a triple grating spectrometer (JY-T64000) equipped with a liquid-nitrogen-cooled CCD detector. The 532 nm laser excitation line was used from a diode pump solid state laser. The  $B_{1g}$  (antinodal) geometry has been obtained from cross polarizations at  $45^\circ$  from the Cu-O bond directions. We got an accuracy on the crystallographic axes orientation with respect to the polarizers close to  $2^\circ$ . All the spectra have been corrected for the Bose factor and the instrumental spectral response. Measurements below and above  $T_c$  have been performed using an ARS closed-cycle He cryostat. The laser power at the entrance of the cryostat was maintained below 2 mW to avoid overheating of the crystal estimated to 3 K/mW at 10 K. The crystals were cleaved before measurements.

ARPES measurements were performed at Diamond Light Source at the I05 beamline [39] as well as at BESSY II

(Helmholtz Zentrum Berlin) at the UE112-PGM2b beamline using the “ $^{13}$ -ARPES” end-station [40]. In both cases crystals were cleaved in ultrahigh vacuum to expose mirrorlike surfaces, energy resolution was kept below 5 meV, and photon energies between 20 and 100 eV were used. The photon energy has been carefully selected each time when the intensity of the particular band should have been enhanced in comparison with other features. The photon energy range (50–55 eV) has been selected in order to probe mostly the antibonding band. For the highest resolution measurements the samples were cooled down to the lowest achievable temperatures, i.e., 8 K at Diamond and 1 K at BESSY. The crystals were first measured by Raman and then by ARPES.

### III. SUPERCONDUCTING GAP AND PSEUDOGAP AROUND THE CRITICAL DOPING LEVEL $p \sim 0.22$

Our first venture was to check the consistency of the ARPES and ERS measurements above  $p_c$ .

In the first row of Fig. 1, the antinodal ERS response and the energy distribution curves (EDCs) related to the antibonding band at the antinodes (AN) and the nodes (N)

of the OD 47 K compound ( $p = 0.236$ ) above and below  $T_c$  are displayed. Because ERS spectroscopy is a two particle probe (both occupied and unoccupied states are involved in the ERS process), the energy of the pair breaking peak in the superconducting (SC) Raman spectrum [red/gray curve in Fig. 1(a)] is at twice the SC gap energy. We find  $\Delta_{SC} = 9.2 \pm 0.2$  meV. On the other hand, ARPES is a one-particle probe: solely occupied states are detected. The estimate of the SC gap by ARPES can be deduced from the EDCs in two different ways. Either by measuring the difference in energy (i) between the quasiparticles peaks below and above  $T_c$  or (ii) between the quasiparticle peaks at the nodes (N) and at the antinodes (AN) below  $T_c$ . The EDCs are sufficiently sharp to extract the gap from the peak location directly, without using additional data processing, such as symmetrization. In case (i) [Fig. 1(b)] we find  $\Delta_{SC1} = 9 \pm 1$  meV very close to the SC gap from ERS. In case (ii) [Fig. 1(c)] the SC gap value  $\Delta_{SC2}$  is slightly lower,  $8 \pm 1$  meV. In the light of our uncertainties on these two methods, it is difficult to say whether this difference in the determination of the SC gap is significant or not and further investigations are required to answer this question.

In the second row are reported the Raman response function and the ARPES EDCs of the antibonding band related to the OD 77 K compound ( $p = 0.201$ ). The SC gap  $\Delta_{SC} = 25$  meV deduced from the pair breaking peak location [Fig. 1(d)] and the energy difference between the N and AN quasiparticle peaks  $\Delta_{SC2}$  [Fig. 1(f)] are in remarkably good agreement. Interestingly, there is no way to define the SC gap from the ARPES EDCs above and below  $T_c$  because the PG appearing in the normal state [see Fig. 1(e)] pushes the quasiparticles peak to the same binding energy as the Bogoliubov quasiparticle peak. This clearly contrasts with the EDCs of the OD 47 K compound [Fig. 1(b)] where the quasiparticles peak below and above  $T_c$  are located at different energies. This is the first evidence from our ARPES data that the PG exists at  $p = 0.201$  below  $p_c \approx 0.22$ . The second proof comes from the ERS data. In Fig. 1(d), on the right energy side of the pair breaking peak (PP), a dip in the SC electronic continuum is observable [see Fig. 1(d)], whereas no dip is detected in the SC Raman spectrum of Fig. 1(a). In previous works, we showed this PP-dip structure results from the interplay between the PG and the SC gap, and can be smoothly connected to the PG appearing in the electronic spectrum above  $T_c$  [25,26]. Note that a dip in the EDC of OD 77 K in Fig. 1(e) is also detected while no dip is observed in the EDC of OD 47 K in Fig. 1(b). The origin of the peak-dip and hump detected by ARPES is still under debate. Several scenarios have been proposed: strong electron-boson coupling, bilayer splitting effect, and PG effect [24,43–48]. In view of our results, the PG could also be considered as a possible origin of the peak-dip-hump structure detected in ARPES.

Finally, we bring a third experimental evidence of the presence of the pseudogap below  $p_c$  and its absence above by comparing the N and AN EDCs of OD 47 K and OD 77 K above  $T_c$ . In Fig. 2(a) are displayed the AN (red curve) and N (green curve) measured at  $T = 60$  K. Although the AN and N quasiparticle peaks have different widths, they overlap well. In sharp contrast, the AN and N quasiparticle peak locations related to the OD 77 K compound (measured at 100 K) are

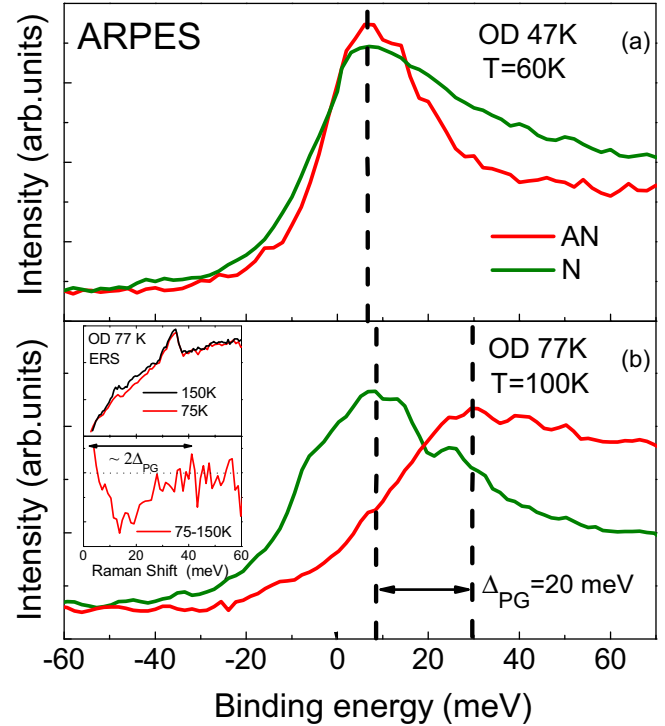


FIG. 2. Antibonding band energy distribution curves at the nodes and antinodes of the overdoped Bi-2212. (a) OD 47 K and (b) OD 77 K compound in the normal state. The inset in (b) displayed (up) the electronic Raman background measured just above  $T_c$  (75 K) and at  $T^*$  (150 K) for the OD 77 K compound; (bottom) the electronic background at 75 K subtracted from the one at 150 K. The energy size of the depletion is approximately 40 meV corresponding (after division par 2) to  $\Delta_{PG} \approx 20$  meV. The peak around 35 meV is a phonon line.

quite distinct [see Fig. 2(b)]. Indeed, close to the Fermi level the PG opens with a loss of low-energy spectral weight at the AN which pushes back the AN peak to higher binding energy in comparison to the N one. The difference in energy (peak to peak) gives  $\Delta_{PG} = 20 \pm 1$  meV which is in the same energy range that the PG gap energy inferred from ERS, see inset of Fig. 2(b). In the top panel of the inset have been reported the Raman electronic backgrounds of OD 77 K at  $T_c$  and  $T^*$ . The subtracted background (bottom of the inset) gives an estimate of the loss of low-energy spectral weight related to the normal state PG. We can then define the energy from which the depletion starts and found to be  $2\Delta_{PG} = 40 \pm 5$  meV. On the contrary, no depletion as the temperature decreases is observed in the Raman spectra of overdoped Bi-2212 compounds with a  $T_c$  below 60 K [13] and *a fortiori* for the OD 47 K compound.

#### IV. CONNECTION BETWEEN THE EXISTENCE OF THE PSEUDOGAP AND THE FERMI SURFACE TOPOLOGY

At this step, our ERS and ARPES investigations show without ambiguity that the PG exists in the Bi-2212 compound at  $p = 0.201$  (related to OD 77 K) and does not exist anymore at  $p = 0.236$  (which corresponds to OD 47 K). These two doping levels are respectively located below and above

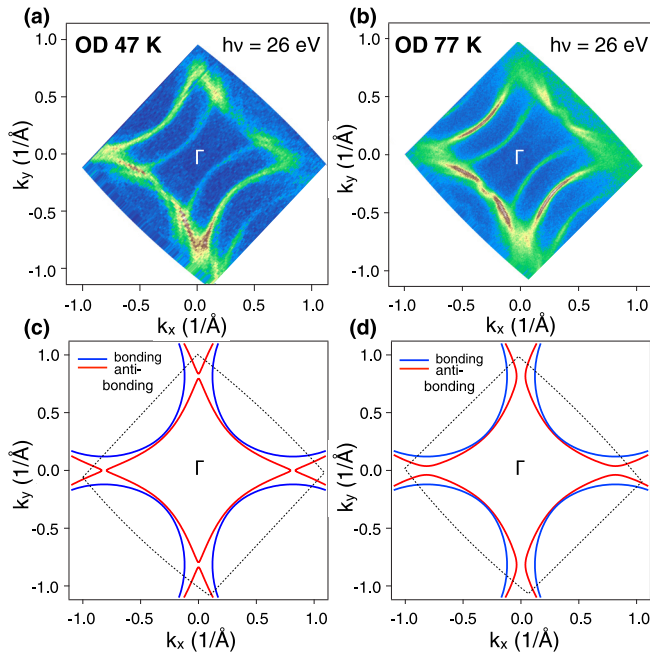


FIG. 3. Fermi surface maps of (a) OD 47 K and (b) OD 77 K compound taken at 8 K using 26 eV photons. Intensity is integrated within a 20 meV window centered at the Fermi level to minimize the influence of the superconducting gap. Results of the tight-binding fit to the experimental data from (c) OD 47 K and (d) OD 77 K samples. Dotted contours in (c) and (d) delimit the Fermi surface area mapped by the ARPES data displayed in (a) and (b). Diffraction replicas are not shown.  $t_{0,0} = 0.416$ ,  $t_{0,1} = t_{1,0} = -0.653$ , and  $t_{1,1} = 0.542$  for bonding bands.  $t_{0,0} = 0.451$  for antibonding bands.  $t_{1,1} = 0.450$ ,  $t_{0,1} = t_{1,0} = -0.630$ , and  $t_{1,1} = 0.463$ ,  $t_{0,1} = t_{1,0} = -0.653$  for OD 47 K and OD 77 K antibonding bands, respectively.

$p_c \approx 0.22$ , the doping level for which we have suggested a change of the Fermi surface topology [13,26]. Now we prove that change of the FS topology actually happens.

In Fig. 3 we compare the spectral weight maps in momentum space at the Fermi level of Bi-2212 for the two doping levels  $p = 0.236$  (OD 77 K) and  $p = 0.201$  (OD 47 K) carried out at essentially the same experimental conditions. We use photon energy at 26 eV to enhance the emission from the antibonding band. Both Fermi surface maps look typical for Bi-2212 showing the diffraction replicas. The latter are the result of the diffraction of the photoelectrons on the topmost layer. It is known that Bi-2212 are approximately 5:1 structurally modulated along the Cu-Cu bonds [49]. Therefore, the primary Fermi surface contours will be replicated, i.e., shifted by approximately one fifth of the Brillouin zone along the diagonal in both directions resulting in the similar but weaker features on the map.

Already a visual comparison of Figs. 3(a) and 3(b) shows that the underlying Fermi surfaces are slightly different. The distance between the  $\Gamma$  point and the Fermi surface contour along the diagonal is larger in the less hole-doped compound, as expected. The main difference, however, is the contour of the antibonding Fermi surface itself. Due to the favorable experimental conditions (photon energy and geometry), this contour is the most intense feature on the maps. In Fig. 3(a) this contour is closed around the  $\Gamma$  point, whereas it is open in Fig. 3(b).

Because of the presence of the superconducting gap in the antinodal region, both Fermi surface contours become smeared-out on the maps, complicating the comparison. This occurs due to the finite integration energy window (20 meV) of the ARPES signal near the Fermi level, which increases the momentum width of the features following the BCS-like bending-back behavior in the superconducting state.

On the other hand, the spectral function at these low temperatures has the sharpest peaks at all binding energies. Using this advantage, we fitted the simple tight-binding model [ $E(k_x, k_y) = t_{0,0} + t_{0,1} \cos(y) + t_{1,0} \cos(x) + t_{1,1} \cos(x) \cos(y)$ ] to both data sets.

We used not only the Fermi surface maps shown in Fig. 3 but also the underlying dispersion in the broad energy interval below the Fermi level not shown here. The fit procedure (involving the tight-binding function with  $k_x, k_y$  and energy as variables) allows us to avoid the immediate vicinity of the Fermi level where the gap bends the features back [50].

The results of the tight-binding fit are presented in Figs. 3(c) and 3(d). They clearly confirm the transition from a holelike antibonding (red contours) Fermi surface in the OD 77 K sample to an electronlike one in the OD 47 K sample.

## V. CONCLUSION

In conclusion, a combined study of ERS and ARPES demonstrates that the PG collapses in between  $p = 0.201$  and  $p = 0.236$  as the FS change of topology from holelike to electronlike in Bi-2212. This is in perfect agreement with a scenario for which the PG ends at a Lifshitz transition which occurs close to  $p_c = 0.22$  in Bi-2212 compound and that the PG only appears on a holelike Fermi surface.

## ACKNOWLEDGMENTS

We are grateful to M. Civelli, I. Paul, M. Ferrero, A. Georges, and L. Taillefer for fruitful discussions. Correspondences and requests for materials should be addressed to A.S. (alain.sacuto@univ-paris-diderot.fr). B.L. is supported by the DIM OxyMORE, Ile de France. S.V.B. is supported by DFG Grant BO 1912/6-1. We acknowledge Diamond Light Source for time on beamline I05 under proposal SI17045.

[1] H. Alloul, T. Ohno, and P. Mendels, *Phys. Rev. Lett.* **63**, 1700 (1989).  
 [2] W. W. Warren, Jr., R. E. Walstedt, G. F. Brennert, R. J. Cava, R. Tycko, R. F. Bell, and G. Dabbagh, *Phys. Rev. Lett.* **62**, 1193 (1989).

[3] C. C. Homes, T. Timusk, D. A. Bonn, R. Liang, and W. N. Hardy, *Phys. C: Superconduct.* **254**, 265 (1995).  
 [4] M. Opel, R. Nemetschek, C. Hoffmann, R. Philipp, P. F. Müller, R. Hackl, I. Tüttó, A. Erb, B. Revaz, E. Walker, H. Berger, and L. Forró, *Phys. Rev. B* **61**, 9752 (2000).

- [5] J. L. Tallon and J. W. Loram, *Phys. C: Superconduct.* **349**, 53 (2001).
- [6] A. A. Kordyuk, S. V. Borisenko, M. S. Golden, S. Legner, K. A. Nenkov, M. Knupfer, J. Fink, H. Berger, L. Forró, and R. Follath, *Phys. Rev. B* **66**, 014502 (2002).
- [7] C. Bernhard, L. Yu, A. Dubroka, K. W. Kim, M. Rössle, D. Munzar, J. Chaloupka, C. T. Lin, and Th. Wolf, *J. Phys. Chem. Solids* **69**, 3064 (2008).
- [8] Y. Kohsaka, C. Taylor, P. Wahl, A. Schmidt, J. Lee, K. Fujita, J. W. Alldredge, K. McElroy, J. Lee, H. Eisaki, S. Uchida, D.-H. Lee, and J. C. Davis, *Nature (London)* **454**, 1072 (2008).
- [9] U. Chatterjee, D. Ai, J. Zhao, S. Rosenkranz, A. Kaminski, H. Raffy, Z. Li, K. Kadowaki, M. Randeria, M. R. Norman, and J. C. Campuzano, *Proc. Natl. Acad. Sci. USA* **108**, 9346 (2011).
- [10] I. M. Vishik, M. Hashimoto, R.-H. He, W.-S. Lee, F. Schmitt, D. Lu, R. G. Moore, C. Zhang, W. Meevasana, T. Sasagawa, S. Uchida, K. Fujita, S. Ishida, M. Ishikado, Y. Yoshida, H. Eisaki, Z. Hussain, T. P. Devereaux, and Z.-X. Shen, *Proc. Natl. Acad. Sci. USA* **109**, 18332 (2012).
- [11] A. Sacuto, Y. Gallais, M. Cazayous, M.-A. Méasson, G. D. Gu, and D. Colson, *Rep. Prog. Phys.* **76**, 022502 (2013).
- [12] S. Sakai, S. Blanc, M. Civelli, Y. Gallais, M. Cazayous, M.-A. Méasson, J. S. Wen, Z. J. Xu, G. D. Gu, G. Sangiovanni, Y. Motome, K. Held, A. Sacuto, A. Georges, and M. Imada, *Phys. Rev. Lett.* **111**, 107001 (2013).
- [13] S. Benhabib, A. Sacuto, M. Civelli, I. Paul, M. Cazayous, Y. Gallais, M. A. Méasson, R. D. Zhong, J. Schneeloch, G. D. Gu, D. Colson, and A. Forget, *Phys. Rev. Lett.* **114**, 147001 (2015).
- [14] B. Fauqué, Y. Sidis, V. Hinkov, S. Pailhès, C. T. Lin, X. Chaud, and P. Bourges, *Phys. Rev. Lett.* **96**, 197001 (2006).
- [15] R. Daou, N. Doiron-Leyraud, D. LeBoeuf, S. Y. Li, F. Laliberté, O. Cyr-Choinière, Y. J. Jo, L. Balicas, J.-Q. Yan, J.-S. Zhou, J. B. Goodenough, and L. Taillefer, *Nat. Phys.* **5**, 31 (2009).
- [16] A. Shekhter, B. J. Ramshaw, R. Liang, W. N. Hardy, D. A. Bonn, F. F. Balakirev, R. D. McDonald, J. B. Betts, S. C. Riggs, and A. Migliori, *Nature (London)* **498**, 75 (2013).
- [17] K. Fujita, C. K. Kim, I. Lee, J. Lee, M. H. Hamidian, I. A. Firmo, S. Mukhopadhyay, H. Eisaki, S. Uchida, M. J. Lawler, E. A. Kim, and J. C. Davis, *Science* **344**, 612 (2014).
- [18] S. Badoux, W. Tabis, F. Laliberté, G. Grissonnanche, B. Vignolle, D. Vignolles, J. Béard, D. A. Bonn, W. N. Hardy, R. Liang, N. Doiron-Leyraud, L. Taillefer, and C. Proust, *Nature (London)* **531**, 210 (2016).
- [19] Y. Sato, S. Kasahara, H. Murayama, Y. Kasahara, E.-G. Moon, T. Nishizaki, T. Loew, J. Porras, B. Keimer, T. Shibauchi, and Y. Matsuda, *Nat. Phys.* **13**, 1074 (2017).
- [20] G.-q. Zheng, P. L. Kuhns, A. P. Reyes, B. Liang, and C. T. Lin, *Phys. Rev. Lett.* **94**, 047006 (2005).
- [21] T. Kondo, R. Khasanov, T. Takeuchi, J. Schmalian, and A. Kaminski, *Nature (London)* **457**, 296 (2009).
- [22] L. Mangin-Thro, Y. Sidis, P. Bourges, S. De Almeida-Didry, F. Giovannelli, and I. Laffez-Monot, *Phys. Rev. B* **89**, 094523 (2014).
- [23] Y. He, A. Yi Yin, M. Zech, A. Soumyanarayanan, M. M. Yee, T. Williams, M. C. Boyer, K. Chatterjee, W. D. Wise, I. Zeljkovic, C. T. T. Takeshi Kondo, H. Ikuta, P. Mistark, R. S. Markiewicz, A. Bansil, S. Sachdev, D. E. W. Hudson, and J. E. Hoffman, *Science* **344**, 608 (2014).
- [24] M. Hashimoto, E. A. Nowadnick, R.-H. He, I. M. Vishik, B. Moritz, Y. He, K. Tanaka, R. G. Moore, D. Lu, Y. Yoshida, M. Ishikado, T. Sasagawa, K. Fujita, S. Ishida, S. Uchida, H. Eisaki, Z. Hussain, T. P. Devereaux, and Z.-X. Shen, *Nat. Mater.* **14**, 37 (2015).
- [25] B. Loret, S. Sakai, Y. Gallais, M. Cazayous, M.-A. Méasson, A. Forget, D. Colson, M. Civelli, and A. Sacuto, *Phys. Rev. Lett.* **116**, 197001 (2016).
- [26] B. Loret, S. Sakai, S. Benhabib, Y. Gallais, M. Cazayous, M. A. Méasson, R. D. Zhong, J. Schneeloch, G. D. Gu, A. Forget, D. Colson, I. Paul, M. Civelli, and A. Sacuto, *Phys. Rev. B* **96**, 094525 (2017).
- [27] F. Venturini, M. Opel, T. P. Devereaux, J. K. Freericks, I. Tüttő, B. Revaz, E. Walker, H. Berger, L. Forró, and R. Hackl, *Phys. Rev. Lett.* **89**, 107003 (2002).
- [28] A. Kaminski, S. Rosenkranz, H. M. Fretwell, M. R. Norman, M. Randeria, J. C. Campuzano, J.-M. Park, Z. Z. Li, and H. Raffy, *Phys. Rev. B* **73**, 174511 (2006).
- [29] A. Ino, C. Kim, M. Nakamura, T. Yoshida, T. Mizokawa, A. Fujimori, Z.-X. Shen, T. Kakeshita, H. Eisaki, and S. Uchida, *Phys. Rev. B* **65**, 094504 (2002).
- [30] T. Yoshida, X. J. Zhou, K. Tanaka, W. L. Yang, Z. Hussain, Z.-X. Shen, A. Fujimori, S. Sahrakorpi, M. Lindroos, R. S. Markiewicz, A. Bansil, S. Komiyama, Y. Ando, H. Eisaki, T. Kakeshita, and S. Uchida, *Phys. Rev. B* **74**, 224510 (2006).
- [31] S. R. Park, Y. Cao, Q. Wang, M. Fujita, K. Yamada, S.-K. Mo, D. S. Dessau, and D. Reznik, *Phys. Rev. B* **88**, 220503(R) (2013).
- [32] C. E. Matt, C. G. Fatuzzo, Y. Sassa, M. Månsson, S. Fatale, V. Bitetta, X. Shi, S. Pailhès, M. H. Berntsen, T. Kurosawa, M. Oda, N. Momono, O. J. Lipscombe, S. M. Hayden, J.-Q. Yan, J.-S. Zhou, J. B. Goodenough, S. Pyon, T. Takayama, H. Takagi, L. Patthey, A. Bendounan, E. Razzoli, M. Shi, N. C. Plumb, M. Radovic, M. Grioni, J. Mesot, O. Tjernberg, and J. Chang, *Phys. Rev. B* **92**, 134524 (2015).
- [33] T. Takeuchi, T. Kondo, T. Kitao, H. Kaga, H. Yang, H. Ding, A. Kaminski, and J. C. Campuzano, *Phys. Rev. Lett.* **95**, 227004 (2005).
- [34] T. Kondo, T. Takeuchi, U. Mizutani, T. Yokoya, S. Tsuda, and S. Shin, *Phys. Rev. B* **72**, 024533 (2005).
- [35] N. Doiron-Leyraud, O. Cyr-Choinière, S. Badoux, A. Ataei, C. Collignon, A. Gourgout, S. Dufour-Beauséjour, F. F. Tafti, F. Laliberté, M.-E. Boulanger, M. Matusiak, D. Graf, M. Kim, J.-S. Zhou, N. Momono, T. Kurosawa, H. Takagi, and L. Taillefer, *Nat. Commun.* **8**, 2044 (2017).
- [36] W. Wu, M. S. Scheurer, S. Chatterjee, S. Sachdev, A. Georges, and M. Ferrero, *Phys. Rev. X* **8**, 021048 (2018).
- [37] H. Bragança, S. Sakai, M. C. O. Aguiar, and M. Civelli, *Phys. Rev. Lett.* **120**, 067002 (2018).
- [38] According to our previous investigations on the Bi-2212 system (see Sec. C of the SM of Ref. [13]), the pair breaking peak energy in the overdoped regime is proportional to  $T_c$ . Once  $T_c$  is determined, the doping value was provided via the Presland and Tallon's equation [51]. According to this equation, a three decimal digits are necessary because a relative  $T_c$  change of 1 K corresponds to a doping level change of 0.001 in the overdoped regime. One can question about the absolute doping value provided by this phenomenological method. However, what matters here is that the samples with two different  $T_c$  larger than 3 K can be clearly identified by the difference of their peak breaking location.

- [39] M. Hoesch, T. K. Kim, P. Dudin, H. Wang, S. Scott, P. Harris, S. Patel, M. Matthews, D. Hawkins, S. G. Alcock, T. Richter, J. J. Mudd, M. Basham, L. Pratt, P. Leicester, E. C. Longhi, A. Tamai, and F. Baumberger, *Rev. Sci. Instrum.* **88**, 013106 (2017).
- [40] S. V. Borisenko, *Synchrotron Rad. News* **25**, 6 (2012).
- [41] R. Liu, M. V. Klein, P. D. Han, and D. A. Payne, *Phys. Rev. B* **45**, 7392 (1992).
- [42] K. C. Hewitt, N. L. Wang, J. C. Irwin, D. M. Pooke, A. E. Pantoja, and H. J. Trodahl, *Phys. Rev. B* **60**, R9943(R) (1999).
- [43] M. Eschrig and M. R. Norman, *Phys. Rev. Lett.* **85**, 3261 (2000).
- [44] A. A. Kordyuk, S. V. Borisenko, T. K. Kim, K. A. Nenkov, M. Knupfer, J. Fink, M. S. Golden, H. Berger, and R. Follath, *Phys. Rev. Lett.* **89**, 077003 (2002).
- [45] S. V. Borisenko, A. A. Kordyuk, T. K. Kim, A. Koitzsch, M. Knupfer, M. S. Golden, J. Fink, M. Eschrig, H. Berger, and R. Follath, *Phys. Rev. Lett.* **90**, 207001 (2003).
- [46] A. Damascelli, Z. Hussain, and Z.-X. Shen, *Rev. Mod. Phys.* **75**, 473 (2003).
- [47] T. Cuk, F. Baumberger, D. H. Lu, N. Ingle, X. J. Zhou, H. Eisaki, N. Kaneko, Z. Hussain, T. P. Devereaux, N. Nagaosa, and Z.-X. Shen, *Phys. Rev. Lett.* **93**, 117003 (2004).
- [48] D. Mou, A. Kaminski, and G. Gu, *Phys. Rev. B* **95**, 174501 (2017).
- [49] S. V. Borisenko, M. S. Golden, S. Legner, T. Pichler, C. Dürr, M. Knupfer, J. Fink, G. Yang, S. Abell, and H. Berger, *Phys. Rev. Lett.* **84**, 4453 (2000).
- [50] V. B. Zabolotnyy, D. V. Evtushinsky, A. A. Kordyuk, T. K. Kim, E. Carleschi, B. P. Doyle, R. Fittipaldi, M. Cuoco, A. Vecchione, and S. V. Borisenko, *J. Electron Spectrosc. Relat. Phenom.* **191**, 48 (2013).
- [51] M. R. Presland, J. L. Tallon, R. G. Buckley, R. S. Liu, and N. E. Flower, *Phys. C* **176**, 95 (1991).